Environmental Science & Technology

Article

Cite This: Environ. Sci. Technol. 2019, 53, 463−474

pubs.acs.org/est

Cardiovascular Effects and Molecular Mechanisms of Bisphenol A and Its Metabolite MBP in Zebrafish

A. Ross Brown,[†,§] Jon M. Green,[†] John Moreman,[†] Lina M. Gunnarsson,[†] Sulayman Mourabit,[†] Jonathan Ball,[†] Matthew J. Winter,[†] Maciej Trznadel,[†] Ana Correia,[†] Christian Hacker,[†] Alexis Perry,[†] Mark E. Wood,[†] Malcolm J. Hetheridge,[†] Richard A. Currie,[‡] and Charles R. Tyler*[,†]

[†]Biosciences, College of Life and Environmental Sciences, University of Exeter, Geoffrey Pope, Stocker Road, Exeter, Devon EX4 4QD, U.K.

[‡]Jealott's Hill International Research Centre, Syngenta, Bracknell, Berkshire RG42 6EY, U.K.

Supporting Information

ABSTRACT: The plastic monomer bisphenol A (BPA) is one of the highest production volume chemicals in the world and is frequently detected in wildlife and humans, particularly children. BPA has been associated with numerous adverse health outcomes relating to its estrogenic and other hormonal properties, but direct causal links are unclear in humans and animal models. Here we simulated measured (1×) and predicted worst-case (10×) maximum fetal exposures for BPA, or equivalent concentrations of its metabolite MBP, using fluorescent reporter embryo-larval zebrafish, capable of quantifying Estrogen Response Element (ERE) activation throughout the body. Heart valves were primary sites for ERE activation by BPA and MBP, and transcriptomic analysis of microdissected heart tissues showed that both chemicals targeted several molecular pathways constituting biomarkers for calcific aortic valve disease (CAVD), including extra-cellular matrix (ECM) alteration. ECM collagen deficiency and impact on heart valve structural integrity were confirmed by histopathology for high-level MBP exposure, and structural defects (abnormal curvature) of the atrio-ventricular valves corresponded with impaired cardiovascular function (reduced ventricular beat rate and blood flow). Our results are the first to demonstrate plausible mechanistic links between ERE activation in the heart valves by BPA's reactive metabolite MBP and the development of valvular-cardiovascular disease states.

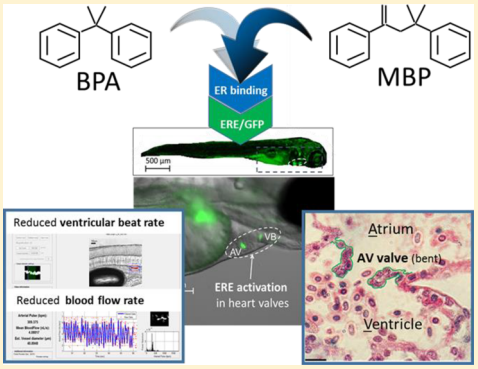

INTRODUCTION

Over 1400 chemicals have been identified as potential endocrine disrupting chemicals (EDCs)[1] with potential to "alter function(s) of the endocrine system and consequently cause adverse health effects in an intact organism, or its progeny, or (sub)populations".[2−5] Over 100 of these chemicals are regarded internationally as priority EDCs and almost half (45%) are estrogenic, that is, estrogen receptor (ER) and/or estrogen-related receptor (ERR) agonists.[6−8] Estrogens play a fundamental role in the formation and function of numerous organs and systems[9] and imbalances are known to increase risks of cancers and disorders of reproductive, nervous, metabolic, immune, and cardiovascular systems in various animal models and humans.[10−14] However, linking cause and effect remains a major challenge in chemical risk/safety assessment. Bisphenol A (BPA) is associated with the above disorders and is one of the world's highest production volume chemicals,[15] to which humans are continually exposed via plastic and other products.[16−23] Reported BPA-effect mechanisms include agonism of nuclear ERs,[24] ERRs,[25,26] membrane ERs,[27,28] epigenetic modulation of estrogen response elements (EREs)[29,30] and weak agonism of androgen and thyroid (T3) receptors.[31,32] Over 2700 peer-reviewed papers have been published on the endocrine effects of BPA (Scopus search, September 2018) illustrating the level of scientific interest in BPA. Despite this high number of studies, 10% of which are in vivo studies, regulatory authorities have concluded that there is insufficient evidence to establish causal links between BPA and adverse effects on human health.[21,33,34] Nevertheless, public pressure has prompted the removal of BPA from baby products in Canada, Europe, and North America,[35,36] due to higher exposures and lower competence for metabolizing BPA in infants.[17,37] Some of the replacement products for BPA are also estrogenic in mammals[38] and fish.[39] Furthermore, the reactive BPA metabolite 4-methyl-2,4-bis(*p*-hydroxyphenyl)pent-1-ene (MBP) has been shown to be far more potent than the parent BPA in terms of: estrogen receptor binding and activation in vitro (×10−1000);[40] stimulation of uterine growth in rats (×500);[41] elevated estrogen receptor (*esr1*) and vitellogenin

Received: August 9, 2018
Revised: November 12, 2018
Accepted: December 6, 2018
Published: December 6, 2018

DOI: 10.1021/acs.est.8b04281
Environ. Sci. Technol. 2019, 53, 463−474

(*vtg1*, *vtg2*) gene and protein expression in medaka (*Oryzias latipes*) (×250−400);[42,43] ERE activation in zebrafish (*Danio rerio*) (×1000) via *esr1*.[44] These findings indicate an urgent need for more integrative test systems capable of evaluating multiple effect levels, linking key molecular events and adverse outcomes for chemicals like BPA and its analogues and metabolites.

Transgenic (TG) zebrafish models offer suitable integrative test systems, whereby key molecular events (e.g., (ant)agonism of hormone receptors, or hormone metabolism) can be identified and quantified by fluorescent protein reporters linked to specific enzymes, receptors or response elements.[45] Spatial and temporal resolution of key molecular events in TG zebrafish can facilitate the detection of chemical effects throughout the body in vivo, in real time[45−49] and can help establish causal links with subsequent adverse effects on biological development and/or function.[39,44] Here we exploit TG(ERE:GFP)Casper zebrafish to study the effects of BPA and its highly estrogenic metabolite MBP on cardiovascular (CV) development and function, building on previous work using this model, which highlighted the heart, and heart valves in particular, as being key targets for these compounds.[39,44,47,48]

MATERIALS AND METHODS

Test Substances. Bisphenol A or BPA: 2,2-bis(4-hydroxyphenyl)propane (99% pure, CAS No. 80−05−7) was obtained from Sigma-Aldrich Company Ltd., Dorset, UK.

The BPA derivative MBP: 4-methyl-2,4-bis(*p*-hydroxyphenyl)pent-1-ene (99% pure, CAS No. 13464−24−9) was synthesized at the University of Exeter (Supporting Information (SI) Figure S1).

Test Organisms. Test organisms were third generation homozygous TG(ERE:GFP)Casper zebrafish (*Danio rerio*),[48] combining a green fluorescent protein (GFP) reporter system for estrogen response element (ERE) activation[45] in a translucent Casper phenotype.[50] This translucent model extends the use of fluorescent reporters to life-stages >5 dpf, which would otherwise gain skin pigmentation that interferes with GFP detection.[48] This is an important feature of the model, as EDC effects may vary both within a tissue and between body tissues at different life-stages.[4,51,52] The life-stages selected for this study represent two key landmarks in CV development: 5 days post fertilization (dpf) marking formation of the endocardial rings (precursors to the heart valve leaflets); 15 dpf marking elongation of the valve leaflets.[53−55] The latter life-stage also corresponds with the depletion of the egg yolk and peaks in metabolism (oxygen consumption) and heart beat rate.[56]

The zebrafish is an established model for biomedical research on CV development, function, and disease,[53,55,57] including heart valve (mal)formation.[58−61] Despite some basic anatomical differences from the human heart,[58,62] the cellular and molecular mechanisms of heart development are highly conserved between zebrafish and humans[55,63] and zebrafish have several major advantages over other vertebrate models. Heart formation (including valvulogenesis and remodelling, outlined in detail in SI Table S1) is completed by 35 dpf,[62,63] but a heartbeat is detectable as early as 1 dpf, with blood circulation beginning soon thereafter.[64] Standard (resting) heart beat rate in 5−15 dpf embryo-larval zebrafish (160−260 beats per minute; bpm) is much closer to resting human fetal heart rate (130−170 bpm) than in rodents (300−600 bpm).[56,65−67] Furthermore, respiration in embryo-larval stages relies mainly on cutaneous diffusion of O_2 and CO_2, rather than transport by convective blood circulation,[68] enabling the in vivo study of late phenotypes of congenital CV malformations, which would be lethal in mammals.[57]

Ethical Statement. All experimental procedures with zebrafish were conducted in accordance with UK Home Office regulations for the use of animals in scientific procedures and followed local ethical review guidelines and approval processes. Water quality was assessed daily (SI Table S2).

Chemical Exposure. TG zebrafish embryos/larvae were exposed in the laboratory from 6 h post fertilization (hpf) to 5 days post fertilization (dpf) or from 6 hpf to 15 dpf, to aqueous concentrations of BPA (solvent (0.5% DMSO) control 0; low 100; high 1000 μg/L) or its metabolite MBP (solvent control 0; low 2.5; high 25 μg/L) in glass 1L aquaria (n = 6 aquaria per exposure treatment), positioned in random order and each containing ∼120 randomly assigned embryos. The lower BPA concentration was expected to represent maximum measured human maternal-fetal-placental unit concentrations of up to 105 ng/g,[69,70] based on bioconcentration factors ranging from 0.25 to 5.7 in larval and adult zebrafish.[39,71,72] Both lower and 10× higher (worst case) BPA concentrations were substantially below maximum tolerable concentrations.[48] MBP exposure concentrations were based on a relative potency of 250× compared to BPA, measured in vivo in juvenile medaka.[43] Stock solutions were prepared by dissolving pure test chemicals in analytical grade dimethyl sulfoxide (DMSO) and then diluting (200×) in 400 mL of embryo culture water[73] to give the desired nominal exposure concentrations in 0.5% DMSO. The pH of stock solutions was checked and adjusted to 7.5, as necessary. For the longer-term (0−15 dpf) exposure, 90% water changes were undertaken every 2 days, after commencing feeding twice a day at 6 dpf with excess <100 μm particulate fish food (ZM000) and with *Artemia salinus* nauplii from 10 dpf. Exposure solutions were maintained at 28 °C, under a 16h:8h light: dark photoperiod cycle with a 15 min dawn/dusk transition.

Concentrations of exposure solutions were measured in three replicate aquaria per exposure treatment at the start and end of each exposure period. Chemical body burden was also measured in whole zebrafish embryo-larvae at 5 dpf, and in composite samples of ×30 hearts extracted from 5 dpf embryos (n = 3 composite samples per treatment). Heart extraction was performed en masse: × 50 larvae per aquarium were disrupted in ice-cold Leibovitz's L-15 Medium (Invitrogen, UK) containing 10% fetal bovine serum, using a 5 mL syringe and 19 gauge needle,[74] and ×30 hearts were isolated using a 30 μm mesh sieve followed by manual sorting in ice-cold Leibovitz's L-15 Medium under a 5× objective on an Olympus SZX16 microscope (Olympus, UK). Fish/hearts were placed in embryo culture water with a terminal dose of anesthetic of 2 mg/mL tricaine methanesulfonate (MS222) at pH 7.5, then dried under vacuum, macerated and extracted in a solution of 80:20 water:acetonitrile containing an internal standard. Details of chromatographic separation and mass spectrometry analysis of BPA and MBP in water and fish tissues are provided in the SI Table S3. The limit of quantitation (LOQ) was 0.05 μg BPA/L and 0.05 μg MBP/L for water, and 0.5 ng BPA/g and 0.5 ng MBP/g for fish tissue. Bioconcentration factors ($BCF_{whole\ body}$ and BCF_{heart}) were calculated based on a mean whole body wet weight of 1200 μg for 5 dpf zebrafish larvae

DOI: 10.1021/acs.est.8b04281
Environ. Sci. Technol. 2019, 53, 463−474

and a ventricle weight of 10% of the whole body weight at 5 dpf.[75]

Following chemical exposure, TG zebrafish larvae were selected randomly from each aquarium and were subject to the following effects analyses, which were conducted at 28 °C.

Quantifying ERE Activation (Estrogenicity). ERE activation was quantified in the atrio-ventricular (AV) and ventricular-bulbus (VB) valves as follows. At 5 and 15 dpf ×6 larvae per replicate aquaria (n = 6) were washed and then anaesthetised in 0.1 mg/mL MS222 at pH 7.5 and mounted in vivo in 1% low melting agarose in embryo culture water with MS222, and then placed into a glass bottom 35 mm dish (MatTek, Ashland, MA). Larvae were orientated right side down and images were obtained using an inverted compound microscope (Zeiss Axio Observer, Cambridge, UK) with a 10× objective, under consistent GFP excitation for a scanning time of 180 ms, using filter set 38 HE: Excitation BP 470/40 nm, Beam splitter FT 495 nm, Emission BP 525/50 nm. GFP expression was quantified as the relative mean pixel intensity of green fluorescence (relative to the solvent control) in a defined region of interest (ROI) encompassing the heart, using ImageJ software.[76]

Histopathology of the Heart and Heart Valve Leaflets. Histopathology of the heart and heart valve leaflets was conducted on ×6 whole zebrafish larvae per replicate aquaria (n = 6) at 5 and 15 dpf, following terminal anesthesia in 2 mg/mL MS222 at pH 7.5, and destruction of the brain. For visible light microscopy, zebrafish were fixed in Bouin's solution (Sigma-Aldrich, Dorset, UK), progressively dehydrated in 70−100% industrial methylated spirits and embedded in paraffin wax. For transmission electron microscopy (TEM), zebrafish were fixed in 2% glutaraldehyde and 2% paraformaldehyde in 0.1 M PIPES buffer (pH 7.2) for 24 h, washed with buffer (3 × 5 min) and postfixed for 1 h in 1% osmium tetroxide (reduced with 1.5% w/v potassium ferrocyanide) in 0.1 M sodium cacodylate buffer (pH 7.2). After a series of washes in deionized water (3 × 5 min) the larvae were subject to in-block staining with 1% uranyl acetate for 30 min, then 3 × 5 min washes with deionized water and then the larvae were dehydrated through an ethanol gradient and embedded in Spurr resin (TAAB Laboratories, Aldermaston, UK). Sagittal sections were obtained through the midline of the atrium and ventricle (to examine the AV valves). For visible light microscopy, serial sections (5 μm) were obtained and placed on glass slides, stained using Masson's trichrome and examined using a Leitz Diaplan light microscope (×10−100) magnification) to assess for structural pathologies (focusing on valvular cells and interstitial extracellular matrix). For TEM, 70 nm ultrathin sections were collected on pioloform-coated EM copper slot grids (Agar Scientific, Stansted, UK) and were analyzed using a JEOL JEM 1400 operated at 120 kV, and images taken (×3000−20 000) magnification with a digital camera (ES 100W CCD, Gatan, Abingdon, UK) to assess for any ultrastructural effects on the heart valves.

Quantifying CV function. Noninvasive video analysis of the heart and dorsal aorta was used to measure multiple cardiovascular (CV) end points simultaneously.[67] At 15 dpf ×6 larvae per replicate aquaria (n = 6), were anaesthetized in 0.1 mg/mL MS222 and embedded right side down in 1% agarose in a single well of a press-to-seal silicon isolator (Sigma-Aldrich, Poole, UK) on a clear microscope slide. The slide was then viewed using an inverted light microscope (Leica DM IRB, Leica Microsystems UK Ltd., Milton Keynes, UK, 5× objective) fitted with two high speed video cameras. The first camera (Grasshopper GRAS-50S5C−C, Richmond, Canada) recorded ventricular heart beat at 30 frames per second (the atrium was obscured at 15 dpf). The second camera recorded blood flow in the dorsal aorta, caudal to the swim bladder, at 120 frames per second (Grasshopper GRAS-03K2M-C, Richmond, Canada). Both cameras were focused independently on their respective regions of interest, to ensure optimal image quality, and set to record simultaneously for 5 min; recordings from the last 3 min were subject to image analysis as follows. Resting (standard) ventricular beat rate (bpm, beats per minute) was measured using MicroZebraLab image analysis software (v3.5, ViewPoint, Lyon, France). Resting (standard) aortic blood flow rate (nL/s) was measured using ZebraBlood (v1.3.2, ViewPoint, Lyon, France).

Quantifying Metabolic Scope. Metabolic scope, combining scope for growth and scope for movement, were measured in terms of specific growth rate (SGR)[77] and critical swimming speed (U_{crit}),[78] respectively. SGR was calculated by measuring individual standard body length (±0.01 mm from snout to caudal peduncle) of TG zebrafish larvae (×10 per aquarium) under anesthetic (0.1 mg/mL MS222) at 5 and 15 dpf, using an Olympus SZX16 microscope and cellSens image analysis software. Since individual fish were not tagged, mean specific growth rate (mean SGR as % standard body length per day) was calculated for each aquarium (eq 1). Critical swimming speed (U_{critb} as standard body lengths/sec) was then assessed at 15 dpf, by placing ×5 larvae at a time in a cylindrical swim flume of length 25 cm, internal diameter 2 cm and volume 78.55 mL, and increasing laminar water flow incrementally by 1.33 cm/sec every 300 s (5 min) until the time to exhaustion for all individual larvae. U_{critb} was calculated based on aquarium-mean standard body length at 15 dpf (eq 2).

Equations.

$$\text{meanSGR} = ((\ln \text{SL @15dpf}) - \ln \text{SL @5dpf})/T) \times 100 \quad (1)$$

Where SL is mean standard length per aquarium (mm); T is time interval (days)

$$U_{critb} = U + (t/t_i \times U_i) \quad (2)$$

Where U is penultimate swimming speed (mean standard body lengths/sec); U_i is velocity increment (1.33 cm/sec); t is time swum in final velocity increment (secs); t_i is time interval for each increment (300 s).

Transcriptomic Profiling of Heart Tissues. Hearts were removed from TG zebrafish larvae following terminal anesthesia in 2 mg/mL MS222 at pH 7.5, followed by destruction of the brain. At 5 dpf ×50 larvae per replicate aquaria (n = 4) were disrupted in ice-cold Leibovitz's L-15 Medium (Invitrogen, UK) containing 10% fetal bovine serum, and hearts were extracted en masse, as described above. Hearts from larvae of 15 dpf were microdissected individually in ice-cold Leibovitz's L-15 Medium using fine tip forceps (Dumont Inox #5SF) and an Olympus SZX16 microscope. Hearts for the 15 dpf larvae were pooled (×30 per aquarium) and then snap frozen in liquid nitrogen. Total mRNA was extracted from each pool of 30 hearts using RNeasy microkits with on-column DNase treatment (Qiagen, UK) and RNA integrity (RIN) scores were confirmed to be in the range 7.4−8.7 using an Agilent 2200 TapeStation (Agilent Technologies Ltd. Berkshire, UK). cDNA libraries were prepared with polyA

DOI: 10.1021/acs.est.8b04281
Environ. Sci. Technol. 2019, 53, 463−474

isolation using Illumina TruSeqTM 2 Stranded mRNA Library Preparation kits and subsequent cluster generation was conducted using TruSeqTM Paired-End Cluster Generation kits (Illumina, San Diego CA). Up to 24 cDNA libraries were prepared for sequencing for each test substance (BPA and MBP): nominally $n = 4$ replicate pooled samples from each of three treatment groups (solvent control, low, high exposure), for two time points (5 dpf and 15 dpf). Libraries were sequenced with 12 per lane using an Illumina HiSeq 2500 in standard mode, generating 100 base pair reads (paired-end).

Statistical Analysis. Prior to statistical analysis, phenotypic data were tested for normality (Anderson−Darling test) and homogeneity of variance (Bartlett's or Levene's tests) using Minitab 16 (Minitab, Coventry, UK). Statistical analysis of phenotypic/functional end points was performed using linear mixed effects (lme) models (R-statistics version 3.3.2, R Foundation for Statistical Computing) and all lme models included aquarium as a random effect. A multivariate MANOVA was used to assess the fixed effect of exposure treatment on cardiovascular function, combining both ventricular heart beat rate and blood flow (using the function "cbind"). Statistical significance ($p < 0.05$) of treatment effects on these and other individual phenotypic end points was also determined by "one-way" comparisons of untransformed heart beat or blood flow data, and lme model fit was measured using the Akaike Information Criterion (AIC). Phenotypic/functional effects data are presented in the text or shown graphically as the mean ±95% confidence interval.

Transcriptomic data were quality-trimmed and filtered (to remove sequencing adapters) and then processed using the TopHat/Cufflinks pipeline,[79] followed by differential gene expression analysis comparing chemical exposure treatments with control treatments using DESeq2 v3.6 and an adjusted p-value of <0.05 set as the false discovery rate.[80]

Gene Set Enrichment Analysis (GSEA) using DAVID v6.8,[81] Enrichr[82] and Reactome v66[83] was conducted on sets of differentially expressed genes (for each chemical exposure treatment) to identify over-represented Gene Ontology (GO) terms for biological processes and functional pathways, including KEGG v88[84] and Reactome v66 pathways[83] referenced to the zebrafish (GRCz10) and the human genome (GRCh38.p12).

Transcription Factor Binding Site (TFBS) motif enrichment analysis was conducted on 5 and 50 kilobase (kB) long DNA flanking sequences both up and downstream of the differentially expressed genes to quantify the potential for estrogen receptor interactions; flanking sequences were retrieved using BioMart from Ensembl v94.[85] Over-represented motifs in each gene set were identified using AME[86] in MEME Suite v5.0.2 (http://meme.nbcr.net). Each gene set was "shuffled" to generate a control gene set (with matched GC content), and enriched TFBS motifs were subsequently identified using the JASPAR 2018 (CORE:vertebrate) database.[87]

Gene groups were considered to be enriched when enrichment scores (EASE scores) were >1.3, and when p-values adjusted for multiple-testing (Benjamini-Hochberg) were <0.1.

RESULTS AND DISCUSSION

Chemical Exposure. Mean measured concentrations of aqueous exposure solutions were 117% and 103% of nominal values for 100 and 1000 μg/L BPA (117 ± 4, 1028 ± 23 μg/L) and 84% and 113% of nominals for 2.5 and 25 μg/L MBP (2.1 ± 0.1, 28.2 ± 0.35), and both sets of controls contained no measurable test chemical (SI Table S4). Mean measured bioconcentration factors for BPA were 5 day $BCF_{whole\ body}$ = 2.5 and 3.8 for 100 and 1000 μg/L BPA exposures, respectively, corresponding with whole body concentrations of ~250 and ~3700 ng/g, which are equivalent to ×2.5 and ×37 maximum human maternal-fetal-placental unit concentrations of 105 ng/g.[69,70] Mean measured 5 day BCF_{heart} = 0.09 for the 1000 μg/L BPA exposure was substantially lower than the corresponding $BCF_{whole\ body}$. The mean measured bioconcentration factor for MBP was: 5 day $BCF_{whole\ body}$ = 27 for the 25 μg/L MBP exposure, corresponding with a whole body concentration of 675 ng/g. MBP was not detectable above the LOQ (0.5 ng/g) in heart tissue, so a 5 day BCF_{heart} could not be determined.

ERE Activation. Exposure to BPA or MBP induced fluorescence from the ERE:GFP reporter in the liver and in the region of interest (ROI) encompassing the heart, specifically in the atrio-ventricular (AV) and the ventricular-bulbus (VB) valves (Figure 1), which is consistent with previous studies.[44,48] Higher fluorescence intensity in the heart/valves was not due to chemical partitioning, since heart tissue concentrations for BPA were more than an order of magnitude lower than in whole body tissue (and the water concentration). Instead, greater ERE activation and fluorescence in the heart valves may be due to tissue-specific expression of different ERs and receptor subtypes. Relative mean fluorescence intensity in the ROI (relative to the solvent control) increased with BPA exposure concentration (100 to 1000 μg/L) from 2.2 ± 0.3 to 31 ± 2 at 5 dpf, and showed a similar concentration-related response, increasing from 15.3 ± 1.1 to 26.9 ± 0.2, at 15 dpf. There was a similar response pattern in relative mean fluorescence intensity in the ROI for MBP, increasing with MBP exposure (2.5 to 25 μg/L) from 34 ± 3 to 54 ± 5 at 5 dpf, and from 3.0 ± 0.4 to 14.6 ± 1.5 at 15 dpf (SI Figure S2). Comparing relative mean fluorescence of MBP versus BPA for the lower-level exposure treatments, which can be assumed to lie on the linear sections of the dose response curves,[44,48] we calculated the relative potency of MBP

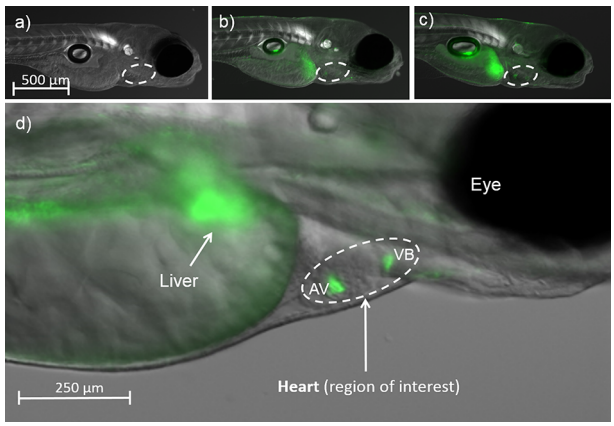

Figure 1. GFP fluorescence locating and quantifying ERE activation by BPA and MBP in the heart in in embryo-larval zebrafish at 5 dpf: (a) Solvent control; (b) 1000 μg/L BPA; (c) 25 μg/L MBP; (d) Close up of the region of interest showing the heart (encircled). Fluorescence indicating Estrogen Response Element (ERE) activation was concentrated in the Atrio-Ventricular (AV) and Ventricular-Bulbous (VB) valves.

DOI: 10.1021/acs.est.8b04281
Environ. Sci. Technol. 2019, 53, 463−474

compared to BPA to be 710× at 5 dpf and 23× at 15 dpf (SI Table S5), which is consistent with results from previous in vivo studies on zebrafish,[39,44] medaka[42,43] and rats.[41]

Greater potency of MBP compared with BPA may be explained, at least in part, by the bioconcentration of MBP from water (5 day $BCF_{whole\ body}$ = 27), which was 1 order of magnitude greater than for BPA. Chemical exposure level- and time- related changes in ERE/GFP expression in zebrafish heart valves are likely to be influenced by range of interacting factors. The lower relative potency of MBP in larvae at 15 dpf, compared with that in 5dpf larvae, followed a net reduction in ERE:GFP fluorescence intensity, possibly corresponding (to some extent) with tissue thickening in older fish. Furthermore, the reduction in fluorescence intensity over time was greater in MBP compared to BPA treatments. These results are consistent with metabolic activation of BPA in fish[42,43,88] and greater metabolic activity in 15 dpf compared to 5 dpf zebrafish larvae.[56] The observed variation in levels of ERE activation at these different life stages may also be due in part to age-related variation in the expression of different ERs and receptor subtypes.[52]

Effects on the Structure of the Heart Valve Leaflets. There was qualitative evidence of ultrastructural changes in the AV valve leaflets in both BPA and MBP high-level exposure treatments at 15 dpf. TEM images (×3000−20 000 magnification) showed the dislocation of valvular cells and the loss of collagen filaments from the interstitial extra-cellular spaces (Figure 2). In the high-level MBP exposure there were also gross-structural changes in the AV valve leaflets. Light microscopy images (×100 magnification), taken following Masson's trichromatic staining, showed that valve leaflets were misshapen (bent) and that the extra-cellular matrix between the bilayer of valvular cells was narrower and lacked collagen (indicated by the lack of blue stain) compared to solvent controls (Figure 2). Although these ultra- and gross- structural effects were clearly evident, they could not be quantified morphometrically, due to the limited number (n = 2 or 3 per treatment) of sagittal sections in which the AV valve leaflets were discernible. No other heart valve pathologies were detected in any other treatment or time point, and there was no evidence of edema to indicate general cardiotoxicity. Histological assessment of ventricular-bulbus (VB) valves was not possible from the sagittal sections taken to assess the AV valves, due to their alternative orientation/alignment.

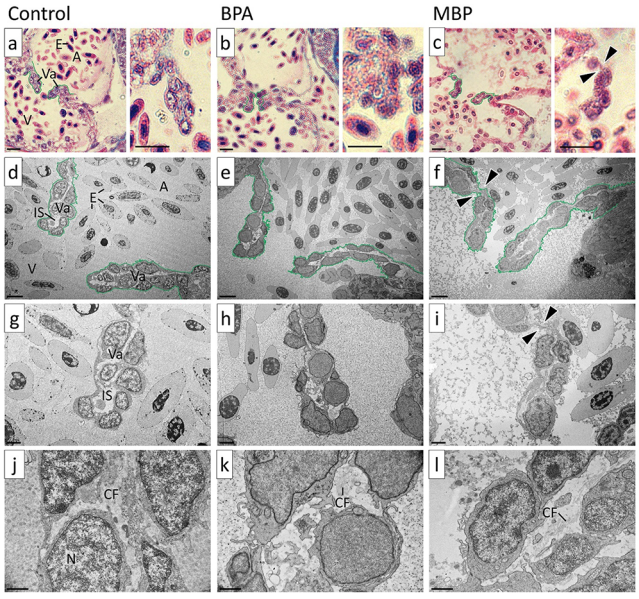

Figure 2. Images of atrio-ventricular (AV) valve leaflets from high-level BPA and MBP exposure treatments versus solvent controls at 15 days post fertilization (dpf) Bright field images a-c are shown at ×100 magnification: AV valve leaflets were bent in the high-level MBP exposure. TEM images d-l are shown at ×3000, ×6000, and ×20 000 magnification: The extra-cellular matrix between the bilayer of valvular cells was narrower and lacked collagen in the high-level BPA and MBP exposure treatments compared to solvent controls (qualitative assessment). Annotations: A = atrium, V = ventricle, E = erythrocytes, Va = valve leaflet, IS = interstitial space, CF = collagen fibers, N = nucleus, arrow heads indicate bent AV valve leaflet. Scale bar (bottom left in each image): a−c = 10 μm; d−f = 5 μm; g−i = 2 μm; j−l = 1 μm.

Effects on CV Function. There were no discernible effects of BPA exposure on CV function in agreement with a previous study,[44] but high-level MBP exposure resulted in a statistically significant reduction (versus solvent controls) in ventricular heart beat rate (218 ± 4 versus 249 ± 7 bpm; p = 0.023) and aortic blood flow rate (1.55 ± 0.07 versus 1.95 ± 0.06 nL/s; p = 0.03) in 15 dpf zebrafish, according to the linear mixed effect model lme(Rate ∼ Treatment, random = ∼1|Tank1) (Figure 3; SI Table S6). These results fall within ranges reported at 28 °C for zebrafish aged 3.5−21 dpf for resting heart beat rate (160−260 bpm)[56,65−67] and resting blood flow rate (500 to 1860 μm/s; equivalent to 0.25−2.1 nL/s).[67,89,90] Ontogeny of embryo-larval development in zebrafish is such that heart beat and blood flow rate vary substantially with development time and peak at 10−20 dpf, a period which corresponds with a peak in aerobic metabolism.[56] Therefore, CV performance is likely to be most critical for our selected life-stage (15 dpf) and reduced CV performance (20% reduction in blood flow rate) could be biologically significant. The proportional reduction in blood flow (20 ± 3.6%) was greater than for heart beat rate (12 ± 2.3%), potentially indicating valve prolapse (although note the variation in these CV parameters). We were unable to observe valve function directly because of tissue thickening, nor were we able to demonstrate AV decoupling as being symptomatic of valve prolapse,[91] since organ growth prevented imaging of both atrial and ventricular beating at 15 dpf. Nevertheless BPA exposures up to 2500 μg/L have been shown to induce erratic AV beat ratios in 5 dpf zebrafish.[44]

Effects on Metabolic Scope. No effects of BPA or MBP were seen on metabolic scope (i.e., SGR and U_{critb}) (SI Figure S3 and Table S7). These energetic measures provide a general indication of individual metabolic scope, that is, energetic reserves beyond basal metabolism.[92] U_{critb} integrates anaerobic as well as aerobic scope for movement[93] and also cardio-respiratory performance.[65] The lack of significant effects (despite downward trends for MBP) may have been due to substantial interindividual variation across the exposure treatments. Interindividual differences in locomotory performance traits have been observed in larval zebrafish between 3 and 21 dpf, and shown to be due to heritable genetic factors not necessarily related to body size.[65] Our test organisms were third generation transgenic zebrafish maintained in up to six spawning groups with 30 fish in each group, therefore genetic variation may have been a confounding factor, but this was not quantified. High interindividual variation may also be related to larval swimming behavior, which is characterized by intermittent bursts of swimming,[94] such that prolonged swim

DOI: 10.1021/acs.est.8b04281
Environ. Sci. Technol. 2019, 53, 463−474

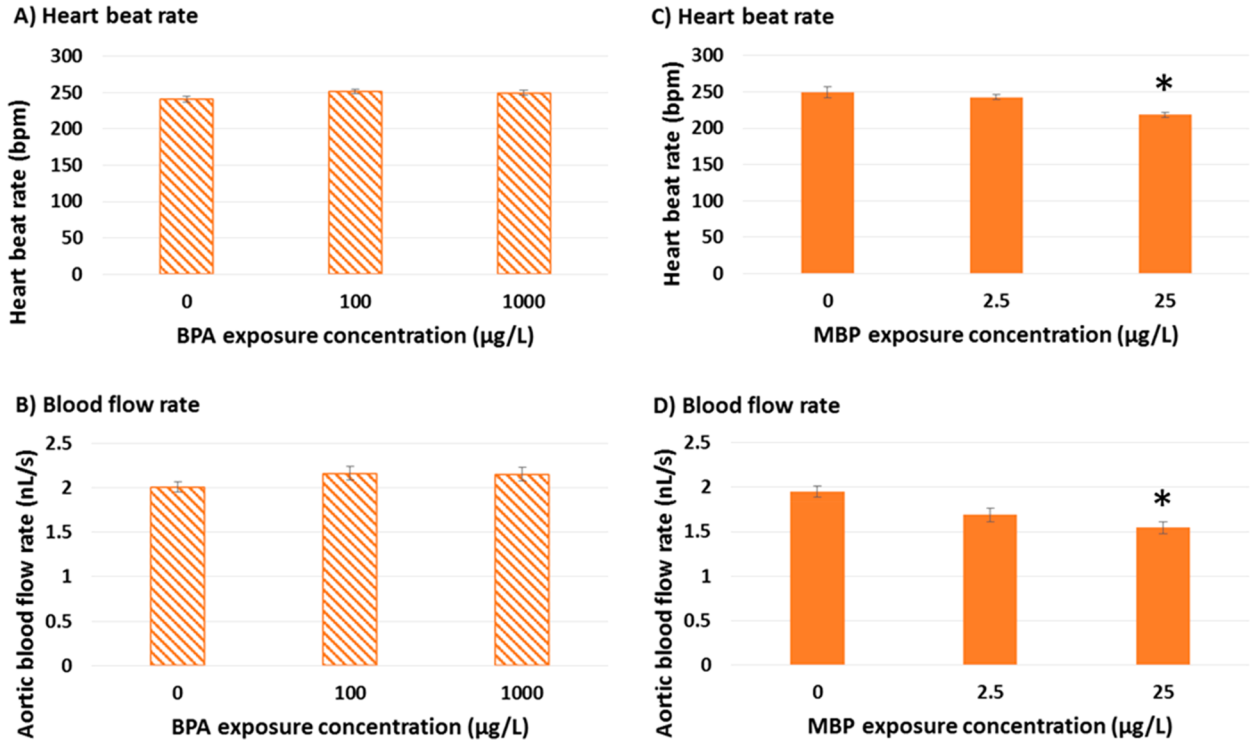

Figure 3. Effects of BPA and MBP exposure on cardiovascular function in zebrafish larvae at 15 days post fertilization (dpf) Hatched bar charts (A-B) represent BPA, solid bar charts (C−D) represent MBP. Data represent six individual fish taken randomly from each of six separate aquaria (n = 6 experimental replicates) per exposure treatment. Bar heights represent means, error bars represent 95% confidence intervals. Significant differences from 0 μg/L solvent control ($p > 0.05$) are highlighted with an asterisk.

challenge tests >10 min may not reliably indicate swimming stamina.[65] Our swim challenge tests typically ran for 5−10 min and mean U_{critb} ranged from 10.7 to 12.6 body lengths/sec, which is comparable to values reported elsewhere, ranging from 13 to 18 body lengths/sec in juvenile and adult zebrafish.[95,96]

Effects on the Heart Transcriptome. BPA (100, 1000 μg/L) and MBP (2.5, 25 μg/L) exposures at 5 and 15 dpf resulted in significant (adjusted p-value < 0.1) differential expression (predominantly down-regulated expression, compared to solvent controls) in a range of genes governing heart valve development and function (SI Figures S4−S5; Tables S8−S10). The down-regulation of a range of genes by ER signaling (via *esr1*, *esr2* and heterodimers of these) has been demonstrated elsewhere in humans and mammalian models.[97,98] The number of genes affected and the level of effect were greatest at 5 dpf for high-level BPA exposure (371 genes: 329 down-regulated by $\log_2$ fold changes of −0.5 to −9), followed by low-level BPA exposure (131 genes: 115 down-regulated by $\log_2$ fold changes of −0.9 to −9) and high-level MBP exposure (127 genes: 101 down-regulated by $\log_2$ fold changes of −2.5 to −9). There was some overlap between high and low-level BPA exposures at 5 dpf, with 62 genes being common to both treatments, whereas only one gene (elastin microfibril interfacer 3 - *emilin3*) was common to both MBP treatments at 5 dpf, due in part to the low number of genes (8 genes) that were differentially expressed in the low-level MBP exposure (SI Figure S6−S7). Collectively, however, the genes affected by both BPA and MBP at 5 dpf shared significant enrichment for molecular pathways concerning (i) nuclear receptor and calcium signaling (estrogen and (para)thyroid), (ii) lipid metabolism, and (iii) extra-cellular matrix (ECM) interactions[99] (Figure 4; SI Figure S8; Tables S8−S10). ECM-related pathways comprising collagen and cartilage formation and organization were particularly prominent for the high-level MBP exposure, and can be related directly to phenotypic effects on the heart valves observed therein. ECM interactions were found to involve Notch signaling (dre04330) and calcium ion binding (GO:0005509) (SI Table S9) which, along with the aforementioned pathways (i-iii), have previously been linked to the progression of calcific aortic valve disease[99,100] (CAVD - fibrosis, and subsequent calcification and thickening of the aortic valves), which affects up to 13% of human populations in the western world[99] (see later discussion). At 15 dpf fewer genes were differentially expressed compared to 5 dpf. Although only five genes overlapped between time points for the high-level BPA exposure treatment (SI Figure S7), there was gene set enrichment for thyroid hormone synthesis (also seen at 5 dpf for MBP) and for estrogen signaling for the 15 dpf high-level BPA exposure (Figure 4). Both hormone signaling pathways have been highlighted in mammalian studies on BPA.[31,101] Overall, gene sets from 15 dpf represented pathways associated with heart function (more so than development), particularly cardiac muscle contraction (SI Tables S8−S9). Four of the 32 genes down-regulated by the high-level BPA exposure at 15 dpf: actinin alpha 3b (*actn3b*); myosin light chain, phosphorylatable, fast skeletal muscle a (*mylpfa*); myosin, heavy polypeptide 2, fast muscle specific (*myhz2*); and troponin I type 2a (skeletal, fast), tandem duplicate 4 (*tnni2a.4*) have previously been identified as potential biomarkers for cardiac disease in animal models, including zebrafish.[102] Low level BPA exposure at 15 dpf led to the differential expression of only gene: apolipoprotein Da, duplicate 2 (*apoda.2* transport protein). The transcriptomic

DOI: 10.1021/acs.est.8b04281
Environ. Sci. Technol. 2019, 53, 463−474

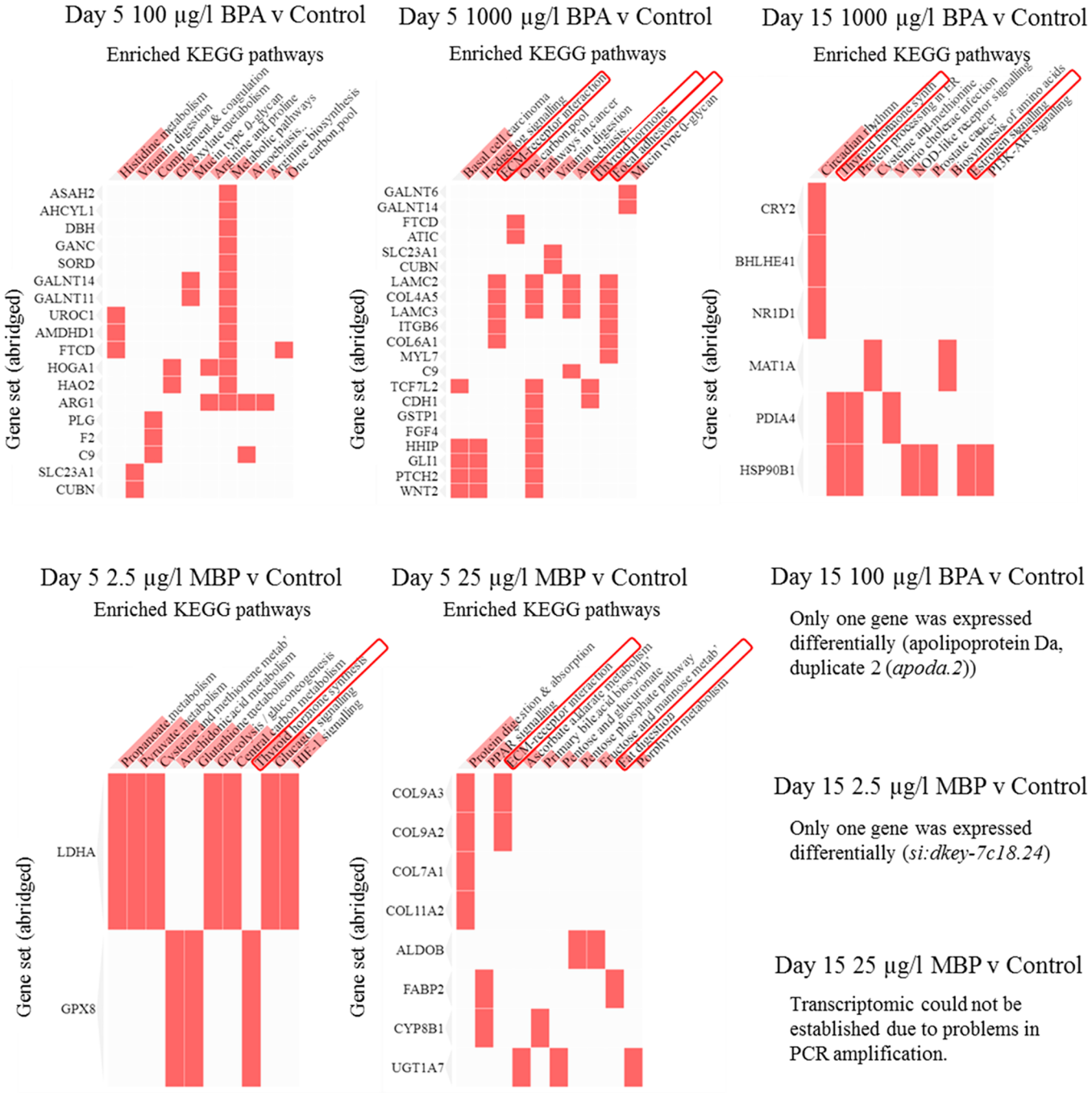

Figure 4. Gene set enrichment for KEGG pathways in heart tissues from 5 and 15 day old larval zebrafish in BPA and MBP exposure treatments (versus solvent controls). Sequence data were generated from hearts pooled from ~30 individuals from each of four separate aquaria (nominally n = 4 experimental replicates) per exposure treatment. Enriched pathways were identified using Enrichr and referenced to the KEGG database (2016). Pathways highlighted in red boxes are calcific aortic valve disease (CAVD) biomarkers. Also see enriched Reactome pathways (in SI Figure S8).

effects of high-level MBP exposure at 15 dpf could not be established due to problems encountered in sample processing (PCR amplification during library preparation), while low-level MBP exposure at 15 dpf led to the differential expression of only one (unannotated) gene (*si:dkey-7c18.24*) (SI Figure S7, Table S8).

Analysis of TFBS motif enrichment showed that differentially expressed genes in both BPA and MBP exposures were similarly enriched and were flanked (within 5 kB) by binding sites for transcription factors associated with estrogen receptor signaling, including: estrogen receptor 2 (*esr2*); specificity proteins constituting ERE tethering factors (*sp1*, *sp3*, *sp4*); pioneer factors facilitating ERE binding (*foxa1*, *nfkb2*, *pbx1*, *runx1*); CAMP responsive element binding proteins (*creb1*, *creb5*) (SI Figure S9, Tables S11−S13). There was also enrichment for estrogen receptors (*esr1*, *esr2*) beyond proximal promoter regions, up to 50 kB from differentially expressed genes (SI Table S13). Examination of these findings versus the established roles of estrogen in normal (and abnormal) heart valve development indicate plausible links between substantial

DOI: 10.1021/acs.est.8b04281
Environ. Sci. Technol. 2019, 53, 463−474

ERE activation by BPA and MBP and the observed transcriptomic and phenotypic effects on the heart valves in our zebrafish. Endogenous estrogen (17β-estradiol) is known to be protective of the CV system in later life, which is one of the reasons for hormone replacement therapy in postmenopausal women. The results of studies on the pathogenesis of CAVD share some similarities with the findings in our study (in terms of effect pathways) and also show that major risk factors include polymorphisms of the estrogen receptor.[103] Inactivation of estrogen receptors is generally associated with increased calcification of the valve leaflets in diseased patients.[104,105] Empirical studies in mammalian models have shown that estrogen inhibits collagen synthesis in rat cardiac fibroblasts[106] and, more specifically, estrogen decreases collagen I and III gene expression in fibroblasts from female rats.[107] BPA has also been shown to cause sex-specific alterations in gene expression profiles, changes in the composition of the cardiac collagen extracellular matrix and altered CV function in CD-1 mice.[101] Furthermore, disruption of collagen in the extracellular matrix has been shown to directly promote valve leaflet calcification in vitro.[108] Based on these studies it is entirely plausible that the estrogenic action of high-level MBP exposure led to collagen deficiency and valve weakening in our larval zebrafish. This preliminary (precalcification) condition resembles "myxomatous degeneration" characterized by collagen degradation and elastic fiber fragmentation, resulting in a "floppy" valve that is prone to prolapse and regurgitation.[109] As with CAVD, it may be speculated that more progressive effects of MBP (and BPA) on heart valve development and function may occur in the longer-term in zebrafish, but this remains to be proven.

Linking Cause and Effect. Although estrogen is known to be cardio-protective in later life, inappropriate estrogenic exposures, including from estrogenic chemicals, in early life, can lead to cardiac malformation.[110] We demonstrate that aqueous exposure to the weak estrogen BPA at 1× and 10× maximum human maternal-fetal-placental unit concentrations, or its more potent metabolite MBP, at equivalent potency concentrations, activate estrogen responsive elements (EREs via estrogen receptor signaling) in the heart valves and alter the expression of a range of genes, including several governing CV development and function in embryo-larval zebrafish. BPA and MBP perturbed similar downstream effect pathways, but only the high-level MBP exposure resulted in gross phenotypic effects including, malformation of the AV valves, and reduced heart beat and blood flow, at 15 dpf. Our findings provide a substantial chain of evidence, but further work is required to fully define adverse outcome pathways for the effects of BPA and its metabolites, including MBP, on heart development and function. Longer-term studies, including lower level chemical exposures, are needed, since heart valve formation and remodelling (e.g., AV valve transitioning from two to four leaflets) is not complete in zebrafish until 35 dpf[62,63] and effects may not become functionally manifest until in later life. Vertebrate models with short life spans, such as zebrafish, are highly amenable for this work.

■ ASSOCIATED CONTENT

Supporting Information

The Supporting Information is available free of charge on the ACS Publications website at DOI: 10.1021/acs.est.8b04281.

Tables describing: zebrafish heart and heart valve morphogenesis (valvulogenesis); water quality; test substance analysis; ERE response - relative mean fluorescence intensity induced by BPA and MBP in the heart valves; effects on CV function; specific growth rate (SGR) and critical swimming speed (U_{critb}); differentially expressed genes and enrichment for GO terms, KEGG and Reactome pathways and TFBS motifs in BPA and MBP exposure treatments. Figures showing: Nuclear Magnetic Resonance Spectrum for MBP; relative fluorescence in ERE-GFP transgenic zebrafish larvae following exposure to BPA and MBP; effects of BPA and MBP exposure on specific growth rate (SGR) and critical swimming speed (U_{critb}); heat maps showing differentially expressed genes; Venn diagrams showing overlap in differentially expressed genes for BPA and for MBP exposure treatments and for time points 5 and 15 dpf; cluster plots showing enrichment of Reactome pathways and TFBS motifs in BPA and MBP exposure treatments (PDF) (XLXS)

■ AUTHOR INFORMATION

Corresponding Author

*(C.R.T.) E-mail: c.r.tyler@exeter.ac.uk; Phone: ++44 1392 724450.

ORCID

A. Ross Brown: 0000-0002-3892-8993

Present Address

§(A.R.B.) Biosciences, College of Life and Environmental Sciences University of Exeter, Lab 201, Geoffrey Pope Building, Stocker Road, Exeter, EX4 4QD, United Kingdom.

Author Contributions

The overall study was designed and implemented by A.R.B., R.C., M.J.H., and C.R.T. A.R.B. ran the study, and analyzed all the data presented in the manuscript; J.M.G. helped to evaluate ERE activation via image analysis of GFP reporters and to measure chemical effects on specific growth rate and critical swimming speed; J.M., L.G., and S.M. helped undertake microdissection of zebrafish hearts, DNA extraction and library preparation for sequencing; J.B. and M.J.W. helped to design and undertake assays to evaluate CV function; M.T. undertook chemical analysis of water and zebrafish embryo-larvae; A.C. and C.H. undertook microscope and TEM work to assess for pathologies of the heart valves, A.P. and M.E.W. synthesized the MBP used in the study; M.J.H., R.A.C., and C.R.T. helped to manage the overall study. The manuscript was written through the contributions of each author, all of whom have given approval to the final version of the manuscript.

Notes

The authors declare no competing financial interest.

■ ACKNOWLEDGMENTS

We are grateful to the anonymous referees whose comments helped to improve the quality of our paper. We are grateful to the Exeter Sequencing Service for undertaking mRNA sequencing, data processing and providing expert guidance on differential gene expression analysis. We are also grateful to Ronny van Aerle for his advice on gene ontology, pathway and motif analysis. This project (and ARB) was funded directly by a BBSRC Flexible Interchange Programme (BB/L01548X/1). Other authors of this work were supported by the following

institutes, organizations and grants: S.M. by NERC (NE/L007371/1), J.M.G. on a BBSRC Industrial CASE research studentship with AstraZeneca Global SHE (ref:620033640), J.M. on a NERC research studentship (ref: 610040829) and LG by AstraZeneca Global SHE Research Programme grant to C.R.T. The sequencing was conducted at the Exeter Sequencing Service, funded by Medical Research Council Clinical Infrastructure award (MR/M008924/1), Wellcome Trust Institutional Strategic Support Fund (WT097835MF), Wellcome Trust Multi User Equipment Award (WT101650MA) and BBSRC LOLA award (BB/K003240/1).

■ ABBREVIATIONS

AIC	Akaike information criterion
AV	atrio-ventricular (valves)
BCF	bioconcentration factor
BPA	bisphenol A
CAVD	calcific aortic valve disease
CV	cardiovascular
DMSO	dimethyl sulfoxide
ECM	extra-cellular matrix
EDC	endocrine disrupting chemical
ER	estrogen receptor
ERE	estrogen response element
GFP	green fluorescent protein
LOQ	limit of quantitation
MBP	4-methyl-2,4-bis(p-hydroxyphenyl)pent-1-ene
PCR	polymerase chain reaction
ROI	region of interest
SGR	specific growth rate
TEM	transmission electron microscopy
TFBS	transcription factor binding site
TG	transgenic
VB	ventricular-bulbus (valves)

■ REFERENCES

(1) TEDX. *TEDX list of potential endocrine disruptors*. 2018; (accessed 26 June 2018): https://endocrinedisruption.org/interactive-tools/tedx-list-of-potential-endocrine-disruptors/.

(2) EC European Commission. *European workshop on the impact of endocrine disrupters on human health and wildlife*. Weybridge, UK. 1996; (accessed 1 February 2018): http://www.iehconsulting.co.uk/IEH_Consulting/IEHCPubs/EndocrineDisrupters/WEYBRIDGE.pdf.

(3) WHO. *IPCS Global assessment of the state-of-the-science of endocrine disruptors* WHO/PCS/EDC/02.2. 2002; (accessed 15 January 2017): http://www.who.int/ipcs/publications/new_issues/endocrine_disruptors/en/.

(4) WHO/UNEP. *State of the science of endocrine disrupting chemicals – 2012. An assessment of the state of the science of endocrine disruptors prepared by a group of experts for the United Nations Environment Programme (UNEP) and World Health Organisation (WHO)*. 2012; (accessed 15 January 2017): http://www.who.int/ceh/publications/endocrine/en/.

(5) EEA European Environment Agency. *Impacts of endocrine disrupters on wildlife, people and their environments*. The Weybridge+15 (1996–2011) report. EEA Technical report No 2/2012, ISSN 1725-2237. 2012; (accessed March 2018): https://www.eea.europa.eu/publications/the-impacts-of-endocrine-disrupters.

(6) EC European Commission. *Endocrine disruptors, strategy, what is being done, priority list*. 2017; (accessed Jan 2018): http://ec.europa.eu/environment/chemicals/endocrine/strategy/being_en.htm.

(7) EPA Environmental Protection Agency. *Endocrine Disruption Screening Program for the 21st Century Dashboard*. 2017; (accessed 10 January 2018): https://actor.epa.gov/edsp21/.

(8) MOE, Ministry of the Environment - Government of Japan. *Endocrine Disrupting Effects of Substances*. 2017; (accessed 2 November 2017): http://www.env.go.jp/en/chemi/ed.html.

(9) Deroo, B. J.; Korach, K. S. Estrogen receptors and human disease. *J. Clin. Invest.* **2006**, *116*(3), 561–570. PMID: 16511588.

(10) Maggi, A.; Ciana, P.; Belcredito, S.; Vegeto, E. Estrogens in the nervous system: mechanisms and nonreproductive functions. *Annu. Rev. Physiol.* **2004**, *66*, 291–313. PMID: 14977405.

(11) Ma, L. Endocrine disruptors in female reproductive tract development and carcinogenesis. *Trends Endocrinol. Metab.* **2009**, *20*(7), 357–363. PMID: 19709900.

(12) EC European Commission. *4th Report on the implementation of the "Community Strategy for Endocrine Disrupters" a range of substances suspected of interfering with the hormone systems of humans and wildlife (COM (1999) 706)*. Commission staff working paper SEC (2011) 1001 final, Brussels. http://ec.europa.eu/environment/chemicals/endocrine/documents/index_en.htm#SubThemes2 (accessed 1 February 2018).

(13) Kortenkamp, A.; Martin, O.; Faust, M.; Evans, R.; McKinlay, R.; Orton, F.; Rosivatz, E. *State of the art assessment of endocrine disrupters*. Final Report to the European Commission Project Contract Number 070307/2009/550687/SER/D3. 2011; URL (accessed March 2018): http://ec.europa.eu/environment/chemicals/endocrine/pdf/sota_edc_final_report.pdf.

(14) Murphy, E.; Kelly, D. P. Estrogen signalling and cardiovascular disease. *Circ. Res.* **2011**, *109*(6), 687–696. PMID: 21885836.

(15) MRC, Merchant Research & Consulting. *Bisphenol A (BPA): 2014 World Market Outlook and Forecast up to 2018*. Market Publishers Ltd. 2014; (accessed 7 December 2017): http://www.prweb.com/releases/2014/04/prweb11761146.htm.

(16) Calafat, A. M.; Ye, X.; Wong, L. Y.; Reidy, J. A.; Needham, L. L. Exposure of the U.S. population to bisphenol A and 4-tertiary-octylphenol: 2003–2004. *Environ. Health Perspect.* **2008**, *116*(1), 39–44. PMID: 18197297.

(17) US NTP-CERHR - National Toxicology Program *Center for the Evaluation of Risks to Human Reproduction. NTP-CERHR Monograph on the potential human reproductive and developmental effects of bisphenol A; 2008*. NIH Publication no: 80–5994. URL (accessed 20 April 2018): www.cerhr.niehs.nih.gov/chemicals/bisphenol/bisphenol.pdf.

(18) Melzer, D.; Rice, N. E.; Lewis, C.; Henley, W. E.; Galloway, T. S. Association of urinary bisphenol a concentration with heart disease: evidence from NHANES 2003/06. *PLoS One* **2010**, *5*(1), e8673. PMID: 20084273.

(19) FAO/WHO Food and Agriculture Organisation/World Health Organisation. *Joint FAO/WHO expert meeting to review toxicological and health aspects of bisphenol A: final report, including report of stakeholder meeting on bisphenol A*, 1–5 November 2010, Ottawa, Canada. Publ. WHO, Geneva, Switzerland, 2011 (accessed 1 September 2016): http://apps.who.int/iris/bitstream/10665/44624/1/97892141564274_eng.pdf?ua=1.

(20) Careghini, A.; Mastorgio, A. F.; Saponaro, S.; Sezenna, E.; Bisphenol, A. nonylphenols, benzophenones, and benzotriazoles in soils, groundwater, surface water, sediments, and food: a review. *Environ. Sci. Pollut. Res.* **2015** *22*(8), 5711–41. PMID: 25548011.

(21) EFSA, CEF Panel (EFSA Panel on Food Contact Materials *Enzymes, Flavourings and Processing Aids). Draft Scientific Opinion on the risks to public health related to the presence of bisphenol A (BPA) in foodstuffs. European Food Safety Authority (EFSA)*, Parma, Italy. 2014; (accessed 1 September 2016): https://www.efsa.europa.eu/sites/default/files/consultation/140117.pdf.

(22) EFSA, CEF Panel (EFSA Panel on Food Contact Materials, Enzymes, Flavourings and Processing Aids). Scientific Opinion on the risks to public health related to the presence of bisphenol A (BPA) in foodstuffs: executive summary. *EFSA J.* **2015**, *13*(1), 3978.

(23) Corrales, J.; Kristofco, L. A.; Steele, W. B.; Yates, B. S.; Breed, C. S.; Williams, E. S.; Brooks, B. W. Global assessment of bisphenol A in the environment: review and analysis of its occurrence and

DOI: 10.1021/acs.est.8b04281
Environ. Sci. Technol. 2019, 53, 463–474

bioaccumulation. *Dose-Response* **2015**, *13*(3) PMID: 26674671, 155932581559830.
(24) Welshons, W. V.; Thayer, K. A.; Judy, B. M.; Taylor, J. A.; Curran, E. M.; vom Saal, F. S. Large effects from small exposures. I. Mechanisms for endocrine-disrupting chemicals with estrogenic activity. *Environ. Health Perspect.* **2003**, *111*, 994−1006. PMID: 12826473.
(25) Okada, H.; Tokunaga, T.; Liu, X.; Takayanagi, S.; Matsushima, A.; Shimohigashi, Y. Direct evidence revealing structural elements essential for the high binding ability of bisphenol A to human estrogen-related receptor-gamma. *Environ. Health Perspect.* **2008**, *116*(1), 32−38. PMID: 18197296.
(26) Tohmé, M.; Prud'homme, S. M.; Boulahtouf, A.; Samarut, E.; Brunet, F.; Bernard, L.; Bourguet, W.; Gibert, Y.; Balaguer, P.; Laudet, V. Estrogen-related receptor γ is an in vivo receptor of bisphenol A. *FASEB J.*. **2014**;*28*(7):3124−3133. PMID: 24744145.
(27) Wozniak, A. L.; Bulayeva, N. N.; Watson, C. S. Xenoestrogens at picomolar to nanomolar concentrations trigger membrane estrogen receptor-alpha-mediated Ca2+ fluxes and prolactin release in GH3/B6 pituitary tumor cells. *Environ. Health Perspect.* **2005**, *113*(4), 431−439. PMID: 15811834.
(28) Sheng, Z. G.; Huang, W.; Liu, Y. X.; Zhu, B. Z. Bisphenol A at a low concentration boosts mouse spermatogonial cell proliferation by inducing the G protein-coupled receptor expression. *Toxicol. Appl. Pharmacol.*. **2012**, *267*(1), 88−94. PMID: 23274518. .
(29) Bromer, J. G.; Zhou, Y.; Taylor, M. B.; Doherty, L.; Taylor, H. S. Bisphenol-A exposure in utero leads to epigenetic alterations in the developmental programming of uterine estrogen response. *FASEB J.*. 2010, *24*(7), 2273−2280. PMID: 20181937.
(30) Mileva, G.; Baker, S. L.; Konkle, A. T.; Bielajew, C. Bisphenol-A: epigenetic reprogramming and effects on reproduction and behavior. *Int. J. Environ. Res. Public Health*. **2014**, *11*(7), 7537−7561. PMID: 25054232.
(31) Moriyama, K.; Tagami, T.; Akamizu, T.; Usui, T.; Saijo, M.; Kanamoto, N.; Hataya, Y.; Shimatsu, A.; Kuzuya, H.; Nakao, K. Thyroid hormone action is disrupted by bisphenol A as an antagonist. *J. Clin. Endocrinol. Metab.* **2002**, *87*, 5185−5190. PMID: 12414890.
(32) Lee, H. J.; Chattopadhyay, S.; Gong, E. Y.; Ahn, R. S.; Lee, K. Antiandrogenic effects of bisphenol A and nonylphenol on the function of androgen receptor. *Toxicol. Sci.* **2003**, *75*(1), 40−46. PMID: 12805653.
(33) US EPA (Environmental Protection Agency). *Bisphenol A (CASRN 80−05−7) Action Plan, 3/29/2010*, 2010; (accessed 20 April 2018): https://www.epa.gov/sites/production/files/2015-09/documents/bpa_action_plan.pdf.
(34) EC JRC, European Commission Joint Research Centre. *Summary dossier review: Bisphenol A-DRAFT-JRC-2015*, 2015; (accessed 30 November 2017): https://circabc.europa.eu/…/Summary%20dossier%20review_Bisphenol%20A-DRAFT.
(35) Health Canada. *Bisphenol A: Update on the Food Directorate's risk management commitments for infant formula*. December 15, 2014; (accessed 1 December 2017): http://www.hc-sc.gc.ca/fn-an/alt_formats/pdf/securit/packag-emball/bpa/bpa-formula-nourrissons-eng.pdf.
(36) FDA Food and Drug Administration. *Update on Bisphenol A (BPA) for Use in Food Contact Applications*, Updated November 2014; (accessed 1 September 2016): http://www.fda.gov/food/ingredientspackaginglabeling/foodadditivesingredients/ucm064437.htm.
(37) Health Canada. Significant New Activity Notice No. 15290 (Section 85 of the Canadian Environmental Protection Act, 1999) Publication of final decision on the screening assessment of a substance − Phenol, 4,4'-(1-methylethylidene)bis-(bisphenol A),CASNo. 80−05−7 − specified on the Domestic Substances List [subsection 77(6) of the Canadian Environmental Protection Act, 1999]; *Canada Gazette* 2008;*142*(42); (accessed 7 November 2017): www.canadagazette.gc.ca/partI/2008/20081018/html/notice-e.html#d101.
(38) Usman, A.; Ahmad, M. From BPA to its analogues: Is it a safe journey? *Chemosphere* **2016**, *158*, 131−142. PMID: 27262103.
(39) Moreman, J.; Lee, O.; Trznadel, M.; David, A.; Kudoh, T.; Tyler, C. R. Acute toxicity, teratogenic, and estrogenic effects of bisphenol A and its alternative replacements bisphenol S, bisphenol F, and bisphenol AF in zebrafish embryo-larvae. *Environ. Sci. Technol.* **2017**, *51*(21), 12796−12805. PMID: 29016128.
(40) Yoshihara, S.; Mizutare, T.; Makishima, M.; Suzuki, N.; Fujimoto, N.; Igarashi, K.; Ohta, S. Potent estrogenic metabolites of bisphenol a and bisphenol b formed by rat liver s9 fraction: their structures and estrogenic potency. *Toxicol. Sci.* **2004**, *78*, 50−59. PMID: 14691209.
(41) Okuda, K.; Takiguchi, M.; Yoshihara, S. *In vivo* estrogenic potential of 4-methyl-2,4-bis(4-hydroxyphenyl)pent-1-ene, an active metabolite of bisphenol A, in uterus of ovariectomized rat. *Toxicol. Lett.* **2010**, *197*, 7−11. PMID: 20435109.
(42) Yamaguchi, A.; Ishibashi, H.; Kohra, S.; Arizono, K.; Tominaga, N. Short-term effects of endocrine-disrupting chemicals on the expression of estrogen-responsive genes in male medaka (*Oryzias latipes*). *Aquat. Toxicol.* **2005**, *72*, 239−249. PMID: 15820104.
(43) Ishibashi, H.; Watanabe, N.; Matsumura, N.; Hirano, M.; Nagao, Y.; Shiratsuchi, H.; Kohra, S.; Yoshihara, S.; Arizono, K. Toxicity to early life stages and an estrogenic effect of a bisphenol A metabolite, 4-methyl-2,4-bis(4-hydroxyphenyl)pent-1-ene on the medaka (*Oryzias latipes*). *Life Sci.*. **2005**, *77*, 2643−2655. PMID: 15961118.
(44) Moreman, J.; Takesono, A.; Trznadel, M.; Winter, M. J.; Perry, A.; Wood, M. E.; Rogers, N. J.; Kudoh, T.; Tyler, C. R. Estrogenic mechanisms and cardiac responses following early life exposure to Bisphenol A (BPA) and its metabolite 4-methyl-2,4-bis(p-hydroxyphenyl)pent-1-ene (MBP) in zebrafish. *Environ. Sci. Technol.* **2018**, *52*(11), 6656−6665. PMID: 29738667.
(45) Lee, O.; Takesono, A.; Tada, M.; Tyler, C. R.; Kudoh, T. Biosensor zebrafish provide new insights into potential health effects of environmental estrogens. *Environ. Health Perspect.* **2012**, *120*(7), 990−996. PMID: 22510978.
(46) Brion, F.; Le Page, Y.; Piccini, B.; Cardoso, O.; Tong, S.-K.; Chung, B. C.; Kah, O. Screening estrogenic activities of chemicals or mixtures *in vivo* using transgenic (*cyp19a1b*-GFP) zebrafish embryos. *PLoS One* **2012**, *7*(5), e36069. PMID: 22586461.
(47) Gorelick, D. A.; Iwanowicz, L. R.; Hung, A. L.; Blazer, V. S.; Halpern, M. E. Transgenic zebrafish reveal tissue-specific differences in estrogen signalling in response to environmental water samples. *Environ. Health Perspect.* **2014**, *122*(4), 356−362. PMID: 24425189.
(48) Green, J. M.; Metz, J.; Lee, O.; Trznadel, M.; Takesono, A.; Brown, A. R.; Owen, S. F.; Kudoh, T.; Tyler, C. R. High-content and semi-automated quantification of responses to estrogenic chemicals using a novel translucent transgenic zebrafish. *Environ. Sci. Technol.* **2016**, *50*(12), 6536−6545. PMID: 27227508.
(49) Green, J. M.; Lange, A.; Scott, A.; Trznadel, M.; Wai, H. A.; Takesono, A.; Brown, A. R.; Owen, S. F.; Kudoh, T.; Tyler, C. R. Early life exposure to ethinylestradiol enhances subsequent responses to environmental estrogens measured in a novel transgenic zebrafish. *Sci. Rep.* **2018**, *8* (1), 2699. PMID: 29426849.
(50) White, R. M.; Sessa, A.; Burke, C.; Bowman, T.; LeBlanc, J.; Ceol, C.; Bourque, C.; Dovey, M.; Goessling, W.; Burns, C. E.; Zon, L. I. Transparent adult zebrafish as a tool for *in vivo* transplantation analysis. *Cell Stem Cell*. **2008**, *2*(2), 183−189. PMID: 18371439.
(51) vom Saal, F. S.; Akingbemi, B. T.; Belcher, S. M.; Birnbaum, L. S.; Crain, D. A.; Eriksen, M.; Farabollini, F.; Guillette, L. J., Jr; Hauser, R.; Heindel, J. J.; Ho, S. M.; Hunt, P. A.; Iguchi, T.; Jobling, S.; Kanno, J.; Keri, R. A.; Knudsen, K. E.; Laufer, H.; LeBlanc, G. A.; Marcus, M.; McLachlan, J. A.; Myers, J. P.; Nadal, A.; Newbold, R. R.; Olea, N.; Prins, G. S.; Richter, C. A.; Rubin, B. S.; Sonnenschein, C.; Soto, A. M.; Talsness, C. E.; Vandenbergh, J. G.; Vandenberg, L. N.; Walser-Kuntz, D. R.; Watson, C. S.; Welshons, W. V.; Wetherill, Y.; Zoeller, R. T. Chapel Hill bisphenol A expert panel consensus statement: integration of mechanisms, effects in animals and potential

DOI: 10.1021/acs.est.8b04281
Environ. Sci. Technol. 2019, 53, 463−474

to impact human health at current levels of exposure. *Reprod. Toxicol.* **2007**, *24*(2), 131−138. PMID: 17768031.
(52) Bondesson, M.; Hao, R.; Lin, C. Y.; Williams, C.; Gustafsson, J.-Å. Estrogen receptor signalling during vertebrate development. *Biochim. Biophys. Acta, Gene Regul. Mech.* **2015**, *1849*(2), 142−151. PMID: 24954179.
(53) Bartman, T.; Walsh, E. C.; Wen, K. K.; McKane, M.; Ren, J.; Alexander, J.; Rubenstein, P. A.; Stainier, D. Y. Early myocardial function affects endocardial cushion development in zebrafish. *PLoS Biol.*. **2004**, *2*(5), E129. PMID: 15138499.
(54) Martin, R. T.; Bartman, T. Analysis of heart valve development in larval zebrafish. *Dev. Dyn.* **2009**, *238*(7), 1796−1802. PMID: 19449301.
(55) Staudt, D.; Stainier, D. Uncovering the molecular and cellular mechanisms of heart development using the zebrafish. *Annu. Rev. Genet.* **2012**, *46*, 397−418. PMID: 22974299.
(56) Barrionuevo, W. R.; Burggren, W. W. O_2 consumption and heart rate in developing zebrafish (*Danio rerio*): influence of temperature and ambient O2. *Am. J. Physiol.* **1999**, *276*(2 Pt 2), R505−13. PMID: 9950931.
(57) Chávez, M. N.; Aedo, G.; Fierro, F. A.; Allende, M. L.; Egaña, J. T. Zebrafish as an emerging model organism to study angiogenesis in development and regeneration. *Front. Physiol.* **2016**, *8*, 7, 56. PMID: 27014075.
(58) Grimes, A. C.; Stadt, H. A.; Shepherd, I. T.; Kirby, M. L. Solving an enigma: Arterial pole development in the zebrafish heart. *Dev. Biol.* **2006**, *290*(2), 265−276. PMID: 16405941.
(59) Hove, J. R., Koster, R. W.; Forouhar, A. S.; Acevedo-Bolton, G.; Fraser, S. E.; Gharib, M. Intracardiac fluid forces are an essential epigenetic factor for embryonic cardiogenesis. *Nature* **2003**, *421*, 172 -177. PMID: 12520305.
(60) Chen, I. H.; Wang, H. H.; Hsieh, Y. S.; Huang, W. C.; Yeh, H. I.; Chuang, Y. J. PRSS23 is essential for the Snail-dependent endothelial-to-mesenchymal transition during valvulogenesis in zebrafish. *Cardiovasc. Res.* **2013**, *97*(3):443−453. PMID: 23213106.
(61) Vermot, J.; Forouhar, A. S.; LieblingM, Wu D.; Plummer, D.; Gharib, M.; Fraser, S. E. Reversing blood flows act through *klf2a* to ensure normal valvulogenesis in the developing heart. *PLoS Biol.*. **2009**, *7*(11), e1000246. PMID: 19924233.
(62) Sarmah, S.; Marrs, J. A. Zebrafish as a vertebrate model system to evaluate effects of environmental toxicants on cardiac development and function. *Int. J. Mol. Sci.* **2016**, *17*(12), 2123. PMID: 27999267.
(63) Beis, D.; Bartman, T.; Jin, S. W.; Scott, I. C.; D'Amico, L. A.; Ober, E. A.; Verkade, H.; Frantsve, J.; Field, H. A.; Wehman, A.; Baier, H.; Tallafuss, A.; Bally-Cuif, L.; Chen, J. N.; Stainier, D. Y.; Jungblut, B. Genetic and cellular analyses of zebrafish atrioventricular cushion and valve development. *Development* **2005**, *132*, 4193−4204. PMID: 16107477.
(64) Stainier, D. Y.; Lee, R. K.; Fishman, M. C. Cardiovascular development in the zebrafish. I. Myocardial fate map and heart tube formation. *Development* **1993**, *119*, 31−40. PMID: 8275863.
(65) Gore, M.; Burggren, W. W. Cardiac and metabolic physiology of early larval zebrafish (*Danio rerio*) reflects parental swimming stamina. *Front. Physiol.* **2012**, *3*, 35. PMID: 22375123.
(66) De Luca, E.; Zaccaria, G. M.; Hadhoud, M.; Rizzo, G.; Ponzini, R.; Morbiducci, U.; Santoro, M. M. ZebraBeat: A flexible platform for the analysis of the cardiac rate in zebrafish embryos. *Sci. Rep.* **2014 5**, *4*, 4898. PMID 25790189.
(67) Parker, T.; Libourel, P.-A.; Hetheridge, M. J.; Cumming, R. I.; Sutcliffe, T. P.; Goonesinghe, A. C.; Ball, J. S.; Owen, S. F.; Chomis, Y.; Winter, M. J. A multi-endpoint *in vivo* larval zebrafish (*Danio rerio*) model for the assessment of integrated cardiovascular function. *J. Pharmacol. Toxicol. Methods* **2014**, *69*(1), 30−38. PMID: 24140389.
(68) Pelster, B.; Burggren, W. W. Disruption of hemoglobin oxygen transport does not impact oxygen-dependent physiological processes in developing embryos of zebrafish (*Danio rerio*). *Circ. Res.* **1996**, *79*, 358−362. PMID: 8756015.
(69) Ikezuki, Y.; Tsutsumi, O.; Takai, Y.; Kamei, Y.; Taketani, Y. Determination of bisphenol A concentrations in human biological fluids reveals significant early prenatal exposure. *Hum. Reprod.*. **2002**;*17*:2839−2841. PMID: 12407035.
(70) Schonfelder, G.; Wittfoht, W.; Hopp, H.; Talsness, C. E.; Paul, M.; Chahoud, I. Parent bisphenol A accumulation in the human maternal-fetal-placental unit. *Environ. Health Perspect.* **2002**, *110*, A703−A707. PMID: 12417499.
(71) Lindholst, C.; Wynne, P.; Marriott, P.; Pedersen, S.; Bjerregaard, P. Metabolism of bisphenol A in zebrafish (*Danio rerio*) and rainbow trout (*Oncorhynchus mykiss*) in relation to estrogenic response. *Comp. Biochem. Physiol., Part C: Toxicol. Pharmacol.* **2003**,*135*, 169−177. PMID: 12860056.
(72) Fang, Q.; Shi, Q.; Guo, Y.; Hua, J.; Wang, X.; Zhou, B. Enhanced bioconcentration of bisphenol A in the presence of nano-TiO2 can lead to adverse reproductive outcomes in zebrafish. *Environ. Sci. Technol.* **2016**, *50*(2), 1005−1013. PMID: 26694738.
(73) ISO. *Water Quality Sampling, ISO 5667, Part 16. Guidance on Biotesting of Samples*; Wiley-VCH: Weinheim-New York. 1997; *30*, http://www.iso.org (accessed 3 April 2018).
(74) Burns, C. G.; MacRae, C. A. Purification of hearts from zebrafish embryos. *BioTechniques* **2006**, *40*(3), 278−281. PMID: 16568816.
(75) Hu, N.; Sedmera, D.; Yost, H. J.; Clark, E. B. Structure and function of the developing zebrafish heart. *Anat. Rec.* **2000**, *60*(2), 148−57. PMID: 10993952.
(76) Schneider, C. A.; Rasband, W. S.; Eliceiri, K. W. NIH Image to ImageJ: 25 years of image analysis. *Nat. Methods* **2012**, *9*(7), 671−675. PMID: 22930834.
(77) Ricker, W. E. Growth rates and models. In *Fish Physiology, Volume VIII. Bioenergetics and Growth*; Hoar, W. S., Randall, D. J., Brett, J. R., Eds.; Academic Press: New York, NY, 1979; p 677−743.
(78) Brett, J. R. The respiratory metabolism and swimming performance of young sockeye salmon. *J. Fish. Res. Board Can.* **1964**, *21*, 1183−1226.
(79) Trapnell, C.; Roberts, A.; Goff, L.; Pertea, G.; Kim, D.; Kelley, D. R.; Pimentel, H.; Salzberg, S. L.; Rinn, J. L.; Pachter, L. Differential gene and transcript expression analysis of RNA-seq experiments with TopHat and Cufflinks. *Nat. Protoc.* **2012**, *7*, 562−578. PMID: 22383036.
(80) Love, M. I.; Huber, W.; Anders, S. Moderated estimation of fold change and dispersion for RNA-seq data with DESeq2. *Genome Biol.*. **2014**, *15*, 550. PMID: 25516281.
(81) Huang, D. W.; Sherman, B. T.; Lempicki, R. A. Systematic and integrative analysis of large gene 569 lists using DAVID bioinformatics resources. *Nat. Protoc.* **2009**, *4*(1), 44−57. PMID: 19131956.
(82) Kuleshov, M. V.; Jones, M. R.; Rouillard, A. D.; Fernandez, N. F.; Duan, Q.; Wang, Z.; Koplev, S.; Jenkins, S. L.; Jagodnik, K. M.; Lachmann, A.; McDermott, M. G.; Monteiro, C. D.; Gundersen, G. W.; Ma'ayan, A. Enrichr: a comprehensive gene set enrichment analysis web server 2016 update. *Nucleic Acids Res.*. **2016**, *44*, Web Server issue gkw377: W90−W97. PMID: 27141961, W90.
(83) Fabregat, A.; Jupe, S.; Matthews, L.; Sidiropoulos, K.; Gillespie, M.; Garapati, P.; Haw, R.; Jassal, B.; Korninger, F.; May, B.; Milacic, M.; Roca, C. D.; Rothfels, K.; Sevilla, C.; Shamovsky, V.; Shorser, S.; Varusai, T.; Viteri, G.; Weiser, J.; Wu, G.; Stein, L.; Hermjakob, H.; D'Eustachio, P. The Reactome Pathway Knowledgebase. *Nucleic Acids Res.*. **2018**, *4*, 46(D1), D649-D655. PMID: 29145629.
(84) Kanehisa, M.; Furumichi, M.; Tanabe, M.; Sato, Y.; Morishima, K. KEGG: new perspectives on genomes, pathways, diseases and drugs. *Nucleic Acids Res.*. **2017**, *45*, D353−D361. PMID: 27899662.
(85) Ruffier, M.; Kähäri, A.; Komorowska, M.; Keenan, S.; Laird, M.; Longden, I.; Proctor, G.; Searle, S.; Staines, D.; Taylor, K.; Vullo, A.; Yates, A.; Zerbino, D.; Flicek, P. Ensembl core software resources: storage and programmatic access for DNA sequence and genome annotation. *Database* **2017**, bax020 PMID: *201728365736*, .
(86) McLeay, R. C.; Bailey, T. L. Motif Enrichment Analysis: a unified framework and an evaluation on ChIP data. *BMC Bioinf.*. **2010**, *11*, 165. PMID: 20356413.

DOI: 10.1021/acs.est.8b04281
Environ. Sci. Technol. 2019, 53, 463−474

(87) Khan, A.; Fornes, O.; Stigliani, A.; Gheorghe, M.; Castro-Mondragon, J. A.; van der Lee, R.; Bessy, A.; Chèneby, J.; Kulkarni, S. R.; Tan, G.; Baranasic, D.; Arenillas, D. J.; Sandelin, A., Vandepoele, K.; Lenhard, B.; Ballester, B.; Wasserman, W. W.; Parcy, F.; Mathelier, A. JASPAR 2018: update of the open-access database of transcription factor binding profiles and its web framework. *Nucleic Acids Res.*. **2018**, *46*(D1), D260−D266. PMID: 29140473.
(88) Yamaguchi, A.; Ishibashi, H.; Arizono, K.; Tominaga, N. *In vivo* and *in silico* analyses of estrogenic potential of bisphenol analogs in medaka (*Oryzias latipes*) and common carp (*Cyprinus carpio*). *Ecotoxicol. Environ. Saf.* **2015**, *120*, 198−205. PMID: 26086576.
(89) Kwon, H.-B.; Wang, S.; Helker, C. S. M.; Rasouli, S. J.; Maischein, H.-M.; Offermanns, S.; Herzog, W.; Stainier, D. Y. R. *In vivo* modulation of endothelial polarization by Apelin receptor signalling. *Nat. Commun.* **2016**, *7*, 11805. PMID: 27248505.
(90) Fieramonti, L.; Foglia, E. A.; Malavasi, S.; D'Andrea, C.; Valentini, G.; Cotelli, F.; Bassi, A. Quantitative measurement of blood velocity in zebrafish with optical vector field tomography. *J. Biophotonics* **2015**, *8*(1−2), 52−59. PMID: 24339189.
(91) Noseworthy, P. A.; Asirvatham, S. J. The knot that binds mitral valve prolapse and sudden cardiac death. *Circulation* **2015**, *132*(7), 551−552. PMID: 26160860.
(92) Elliott, J. M. The energetics of feeding, metabolism and growth of brown trout (*Salmo trutta* L.) in relation to body weight, water temperature and ration size. *J. Anim. Ecol.* **1976**, *45*(3), 923−948. .
(93) Ejbye-Ernst, R.; Michaelsen, T. Y.; Tirsgaard, B.; Wilson, J. M.; Jensen, L. F.; Steffensen, J. F.; Pertoldi, C.; Aarestrup, K.; Svendsen, J. C. Partitioning the metabolic scope: the importance of anaerobic metabolism and implications for the oxygen- and capacity-limited thermal tolerance (OCLTT) hypothesis. *Conserv. Physiol.* **2016**, *4*(1). PMID: 27293766 cow019.
(94) Bagatto, B.; Pelster, B.; Burggren, W. W. Growth and metabolism of larval zebrafish: effects of swim training. *J. Exp. Biol.* **2001**, *204*, 4335−4343. PMID: 11815657.
(95) Plaut, II; Gordon, M. Swimming metabolism of wild-type and cloned zebrafish *Brachydanio rerio*. *J. Exp. Biol.* **1994**, *194*, 209−223. PMID: 9317659.
(96) Palstra, A. P.; Tudorache, C.; Rovira, M.; Brittijn, S. A.; Burgerhout, E.; van den Thillart, G.; Spaink, H. P.; Planas, J. V. Establishing zebrafish as a novel exercise model: swimming economy, swimming-enhanced growth and muscle growth marker gene expression. *PLoS One* **2010**, *5*(12), e14483. PMID: 21217817.
(97) Welboren, W. J.; Stunnenberg, H. G.; Sweep, F. C.; Span, P. N. Identifying estrogen receptor target genes. *Mol. Oncol.*. **2007**, *1*(2), 138−43. PMID: 19383291.
(98) Arnal, J. F.; Lenfant, F.; Metivier, R.; Flouriot, G.; Henrion, D.; Adlanmerini, M.; Fontaine, C.; Gourdy, P.; Chambon, P.; Katzenellenbogen, B.; Katzenellenbogen, J. Membrane and nuclear estrogen receptor alpha actions: from tissue specificity to medical implications. *Physiol. Rev.*. **2017**, *97*(3), 1045−1087. PMID: 28539435.
(99) Small, A.; Kiss, D.; Giri, J.; Anwaruddin, S.; Siddiqi, H.; Guerraty, M.; Chirinos, J. A.; Ferrari, G.; Rader, D. J. Biomarkers of calcific aortic valve disease. *Arterioscler., Thromb., Vasc. Biol.* **2017**, *37*(4), 623−632. PMID: 28153876.
(100) Rusanescu, G.; Weissleder, R.; Aikawa, E. Notch signaling in cardiovascular disease and calcification. *Curr. Cardiol. Rev.* **2008**, *4*(3): 148−156. PMID: 19936191.
(101) Belcher, S. M.; Gear, R. B.; Kendig, E. L. Bisphenol A alters autonomic tone and extracellular matrix structure and induces sex-specific effects on cardiovascular function in male and female CD-1 mice. *Endocrinology*, **2015**, *156*(3), 882−895. PMID: 25594700.
(102) Forough, R.; Scarcello, C.; Perkins, M. Cardiac biomarkers: a focus on cardiac regeneration. *J. Tehran Heart Cent.* **2011**, *6*(4), 179−86. PMID: 23074366.
(103) Nordström, P.; Glader, C. A.; Dahlen, G.; Birgander, L. S.; Lorentzon, R.; Waldenstrom, A.; Lorentzon, M. Oestrogen receptor alpha gene polymorphism is related to aortic valve sclerosis in postmenopausal women. *J. Intern. Med.* **2003**, *254*, 140−146. PMID: 12859695.
(104) Bosse, Y.; Mathieu, P.; Pibarot, P. Genomics: the next step to elucidate the etiology of calcific aortic valve stenosis. *J. Am. Coll. Cardiol.* **2008**, *51*, 1327−1336. PMID: 18387432.
(105) Elmariah, S.; Mohler, E. R. The pathogenesis and treatment of the valvulopathy of aortic stenosis: Beyond the SEAS. *Curr. Cardiol. Rep.* **2010**, *12*(2), 125−132. PMID: 20425167.
(106) Zhou, L.; Shao, Y.; Huang, Y.; Yao, T.; Lu, L. M. 17β-Estradiol inhibits angiotensin II-induced collagen synthesis of cultured rat cardiac fibroblasts via modulating angiotensin II receptors. *Eur. J. Pharmacol.* **2007**, *567*, 186−192. PMID:17511985.
(107) Petrov, G.; Regitz-Zagrosek, V.; Lehmkuhl, E.; Krabatsch, T.; Dunkel, A.; Dandel, M.; Dworatzek, E.; Mahmoodzadeh, S.; Schubert, C.; Becher, E.; Hampl, H.; Hetzer, R. Regression of myocardial hypertrophy after aortic valve replacement: faster in women? *Circulation* **2010**, *14*, 122(11 Suppl), S23−8. PMID: 20837918.
(108) Rodriguez, K. J.; Piechura, L. M.; Porras, A. M.; Masters, K. S. Manipulation of valve composition to elucidate the role of collagen in aortic valve calcification. *BMC Cardiovasc. Disord.* **2014**, *14*, 29. PMID: 24581344.
(109) Hinton, R. B.; Yutzey, K. E. Heart valve structure and function in development and disease. *Annu. Rev. Physiol.* **2011**, *3*, 29−46. PMID: 20809794.
(110) Hook, E. B. Cardiovascular birth defects and prenatal exposure to female sex hormones: A reevaluation of data reanalysis from a large prospective study. *Teratology* **1994**, *49*, 162−166. PMID: 8059421.

DOI: 10.1021/acs.est.8b04281
Environ. Sci. Technol. 2019, 53, 463−474